

DOI: 10.1002/adfm.200800025

The Role of the Interface in CO Oxidation on Au/CeO₂ Multilayer Nanotowers**

By Zheng Zhou, Steven Kooi, Maria Flytzani-Stephanopoulos,* and Howard Saltsburg*

The CO oxidation reaction is studied in this work using a controlled structure consisting of Au/CeO₂ multilayers, in the form of towers of 10 × 10 μm² base, with layer thicknesses in the nanometer range. This structure is prepared on a 3" Si wafer using reverse photolithography and vapor deposition in an e-beam chamber. The thickness of each layer is of nanometer dimensions and only the edges of the Au and CeO₂ layers are exposed to the reaction gas mixture. The CO oxidation reaction rate is found to scale with the total length of the Au/CeO₂ interfaces for nanotowers with the same total Au and CeO₂ surface areas. TEM and X-ray diffraction (XRD) analyses reveal highly stressed gold films in the nanotowers, the lattice strain being temperature and film thickness dependent. Deactivation with time-on-stream is commensurate with relaxation of the gold films, as measured by a drop in their lattice strain.

1. Introduction

CO oxidation over supported nanoscale Au catalysts has been widely studied both experimentally^[1] and theoretically^[2] since the late 1980s, when gold was found to be active for the CO oxidation reaction at low temperatures.^[3] Although the role of the support materials,^[4,5] particle size of Au,^[5,6] interaction between Au and support,^[7,8] as well as the nature of the active sites,^[9,10] and the oxidation state of Au during the reaction^[11] have been studied extensively, the reaction mechanism has not yet been resolved.^[12]

It has been proposed that for Au supported on non-reducible metal oxides such as SiO₂,^[4,5] and Al₂O₃,^[5] the gold particle size is crucial,^[12] while for Au supported on reducible metal oxides such as TiO₂^[10,13,14] and CeO₂,^[15,16] the interface plays an important role. The hypothesis that only nanoscale Au is required for activity^[6] considers the low-coordinated Au atoms in nanoparticles as the active sites and that the activity is not a result of the electronic structure of the small Au

particles.^[17] However, other studies report that the turnover frequency (TOF) of the CO oxidation reaction is related to the length of the Au/support interface and increases with decrease in size of the Au particles.^[18] It has also been reported that oxygen can adsorb on the support and facilitate the reaction.^[19] A theoretical study proposed that there is charge transfer from the reducible oxide support to gold, which promotes the reaction.^[7] The junction theory of Frost may be used to explain the enhancement by the oxide support as a result of the bending of Fermi-level.^[20] A controlled structure thin film catalyst, comprising a bi-layer Au film supported on TiO₂, was recently shown to be the active structure for CO oxidation,^[10] while 3-D nanoparticles on titania were less active.

However, due to the difficulties in controlling the catalyst structure, there is no direct evidence showing the location of the active sites. The Au surface, the support surface, or the gold/support interface all have been suggested as important for activity. To discriminate among these in this work, we constructed a nanotower structure of alternating layers of gold and ceria (as shown in Fig. 1a) according to the method first described by Zuburtikudis and Saltsburg^[21] to discriminate between the size and interface effects in supported catalysts. These authors showed that the metal with one dimension in the nanometer scale (thickness) exhibited the same size dependence of reaction as nanometer diameter particles. Using the same approach, Chaplin found a strong dependence on the interface length for CO oxidation on Ir/Al₂O₃.^[22] Such a structure allows one to vary the surface area and interfacial length independently by modification of the nanotower geometry. To this effect, one can vary the Au/CeO₂ interface length (by interspacing inert SiO₂ layers) while maintaining the same Au and CeO₂ surface area and layer thickness, the latter simulating a 3-D particle size.

[*] Prof. H. Saltsburg, Prof. M. Flytzani-Stephanopoulos, Z. Zhou
Department of Chemical and Biological Engineering, Tufts University
Medford, MA 02155 (USA)
E-mail: howard.saltsburg@tufts.edu
maria.flytzani-stephanopoulos@tufts.edu

Dr. S. Kooi
Institute for Soldier Nanotechnologies, Massachusetts Institute of
Technology Cambridge, MA 02139 (USA)

[**] This work was supported by NSF under NIRT Grant 0304515. The authors would like to thank Kurt Broderick (Microsystems Technology Laboratories at Massachusetts Institute of Technology) for his help with sample preparation; Dr. Richard Schalek (Center for Nanoscale Systems, Harvard University) and Dr. Yong Zhang (Center for Materials Science and Engineering, Massachusetts Institute of Technology) for their help with the TEM studies.

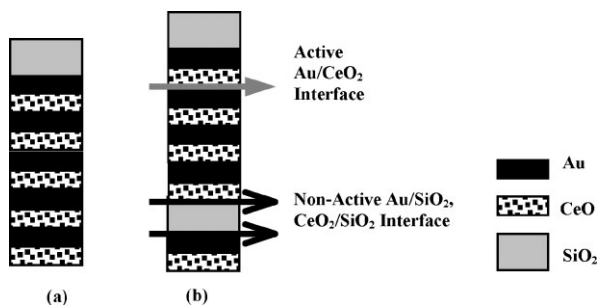


Figure 1. Sketch of a single nanotower Au/CeO₂ with the same Au and CeO₂ surface areas and different number active of interfaces a) 9 and b) 8.

2. Results and Discussion

2.1. Film Structure

As shown in Figure 1, the interfacial length is controlled by inserting inert layers between Au and CeO₂ films, which is only applicable when the film roughness is not changing with its position in the multilayer structure, and, when the side roughness is reproducible. Top roughness was therefore checked for films on the multilayer structure. Despite the different film materials, R_q varied from 2.4 to 2.8 nm from single layer to multilayer structure with variable number of layers. Therefore, the interface length deviation because of the roughness is small. This is also shown in the cross-sectional view of nanotowers (Fig. 3) where the interface can be seen as almost a straight line between any two films, either thin or thick. The quality of pattern is decided partly by the edge line roughness. By optimizing the parameters in photolithography, we obtained reproducible patterns for deposition, which resulted in straight edge lines in the nanotowers, as shown in Figure 2b. The activity for Au/CeO₂ nanotowers with the same structure was reproducible.

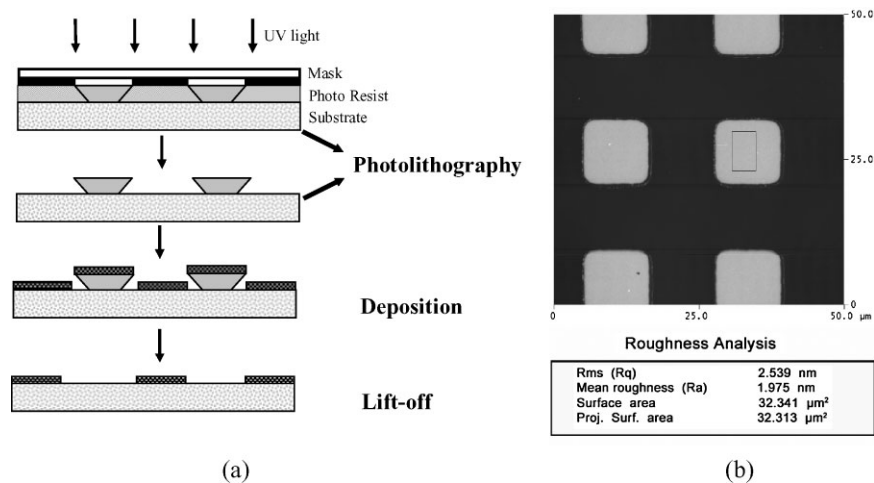


Figure 2. a) Procedure of reverse lithography and deposition; b) top view of developed pattern on a 3" wafer, the features are 10 μm squares, spaced by 10 μm.

Both Au and CeO₂ grow into polycrystalline films as shown in Figure 4. The microstrain of the Au and CeO₂ films was calculated using the (111) crystal planes, which gave the strongest diffraction peaks. The microstrain of the CeO₂ film is about 2%, but neither the microstrain, nor the grain size of CeO₂ in the film varies with respect to the film thickness and heating during the reaction. However, differences were found in the Au film. The thin Au film (4.5 nm) was found more strained than the thick Au film (20 nm). During reaction, about half of the strain was lost, probably due to the heating in the reaction gases,^[25] and this was accompanied by loss of activity.

XRD detects the average change of the film. The film structure was further investigated using TEM to examine the cross-section of the nanotower film properties, such as thickness, continuity of the interface, and local crystallinity. As the specimen must be thin enough for transmission, one must be concerned with possible artifacts that are generated by ion milling. Such artifacts are well known when thin film specimens are prepared using ion beam cutting.^[24] To try to assess the extent of artifact formation, two methods were used here, as described in Section 4: SACT and FIB. Comparing TEM specimens made by SACT and FIB, some differences were found. Figure 3a shows the cross-sectional view of a multilayer film prepared by SACT. Since fewer artifacts are found using this preparation method,^[24] the structure of Figure 3a shows the multilayer structure composed thin films, and is used as reference for the multilayer structure. From the image, one can see that an almost straight interface was formed between Au and CeO₂, and the film thickness is uniform in each layer. However, when FIB was used to prepare the cross-sectional sample, artifacts were evident. When the multilayer film with the same structure was cut using FIB, film growth appears to occur on the top layer and at the left side of the image (Fig. 3b). The deformation of continuous Au films indicates that heating during Ga⁺ beam cutting releases the stress in Au film, which agrees with the release of thin Au film strain during reaction found by XRD. It can be also seen that when the Au film is clamped in the middle of two films, such as the Au layer that is closest to the substrate, no observable deformation is found. Here, the deformed film provides evidence that there was local heating during the FIB process, which was enough to deform the film where the force was poorly balanced.

Although no apparent strain change was found for the 20 nm Au layers after reaction, stress release was found by TEM. As shown in Figure 3c, the Au film buckled up, showing the release of compressive stress^[25] in the direction parallel to the substrate. Accordingly, the film should be under tensile stress in the direction normal to the substrate. Tensile strain has been reported to enhance gold

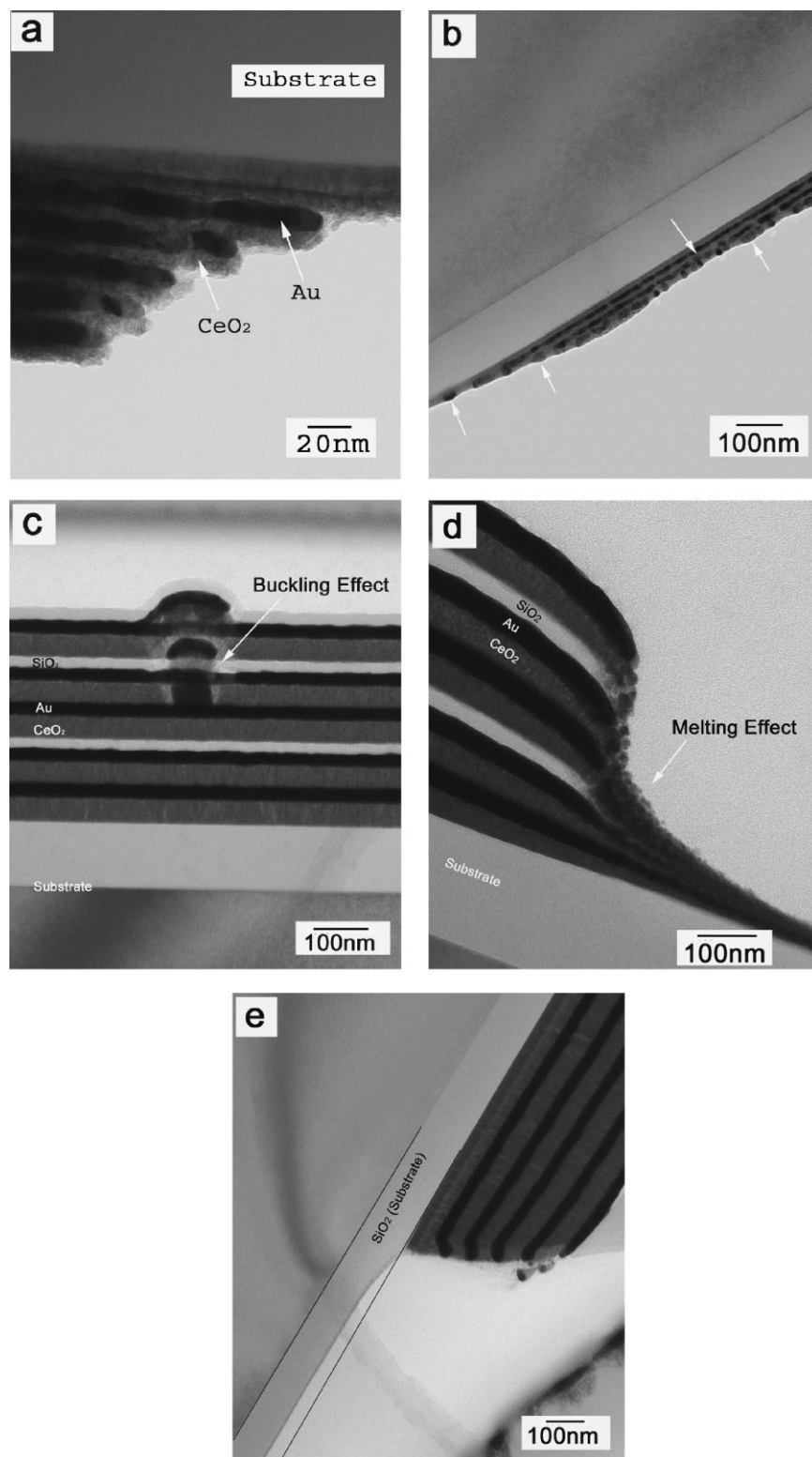


Figure 3. Effect of sample preparation technique to visualize the nanotowers a) prepared using SACT; b)–(d), and e) prepared from FIB. Some of the film deformation points from the ion beam cutting are indicated with arrows. Film thickness: a) and b) 4.5 nm layer⁻¹; c), d), and (e) 20 nm layer⁻¹.

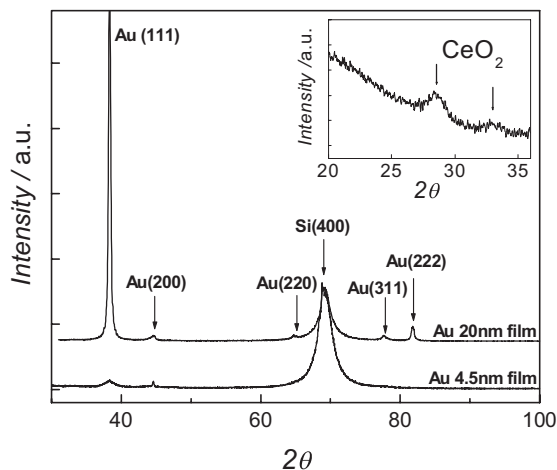
particle reactivity.^[26–28] The sharp boundary between the buckle and the bulk film shows that these defects were not created during deposition because if so, the film would be continuous.

Further stress release is shown at the edge of nanotowers (Fig. 3d), where the highest distortion is expected. The edge of the film is free on one side; so that the film is free to expand upon heating and releases the internal stress, forming a melting curve. Furthermore, the rapid temperature change probably resulted in squeezing particles out of the film. However, the Ar⁺ sputtered edge did not show the melting effect (Fig. 3e). The sputtering direction was normal to the substrate. Using the SiO₂ layer as internal calibration, it is found the thickness sputtered away was around 20 nm, which is thinner than the melted tail shown in Figure 3d. This proves that the Ar⁺ sputtering releases the edge of the nanotowers, preventing deformation during subsequent Ga⁺ beam cutting in preparation of the TEM specimen.

2.2. Activity Measurements

By fixing the surface area of Au and CeO₂, and changing only the Au/CeO₂ interfacial length, one can tell then if the reaction happens at the interface, as activity will change with change of the interface length. Simply dividing the original thick layer into increasingly thinner layers showed an effect of the number of layers/interfaces but this does not rule out a size effect. To resolve this, a modified nanotower structure has been fabricated by inserting an inert layer between Au and CeO₂.

Using the following nanotower structures: (i) a three bi-layer Au/SiO₂ with a SiO₂ cap, and (ii) a three bi-layer CeO₂/SiO₂ with a SiO₂ cap, no CO oxidation activity was detected on either sample upon heating to 200 °C (Fig. 5) confirming the lack of activity of the SiO₂/Au and SiO₂/CeO₂ interfaces and of the Au and CeO₂ surfaces. SiO₂ was used therefore as the inert cap and inter-layer spacer. It is unclear whether the texture of each film could be affected by the presence of SiO₂ because of the difficulties in preparing cross-sectional samples free of artifacts.



Film thickness (nm /layer)	Sample Conditions	Au		Ce	
		Microstrain (%)	Grain size (nm)	Microstrain (%)	Grain size (nm)
4.5	As deposited	1.9	5.47	1.9	6.08
	Used	1	9.37	2.1	6.99
20nm	As deposited	0.4	22.42	2	6.78
	Used	0.38	27.09	2	6.5
20nm	Ar sputtered after deposition	0.5	16.64	1.5	5.11
	Used	0.5	18.18	1.4	6.38

Figure 4. XRD analysis of Au and CeO₂ films.

To test the role of the interfaces in CO oxidation, two Au-CeO₂ nanotowers with the same CeO₂ and Au surface areas were made. One has five Au/CeO₂ interfaces and the other has no Au/CeO₂ interface as all the interfaces were separated with 10 nm SiO₂ layers. The two samples were tested for CO oxidation activity under the same conditions as described above. For nanotowers with five interfaces, CO was completely converted to CO₂ within several minutes. However, for the nanotowers without any Au/CeO₂ interfaces, no conversion of

2.3. Study of the Activity along the Interface

To measure quantitatively the activity with respect to the interface length, a set of nanotowers with five bi-layers of Au (4.5 nm) and CeO₂ (4.5 nm) and different number of interfaces were prepared. Each SiO₂ layer deposited between the Au and CeO₂ films reduces the number of interfaces by one (see Fig. 1b). In these experiments, the number of interfaces varied from 5 to 9, while the thickness of each film and the total surface area of each active component were kept the same. It was found that the activity increases linearly with increase in numbers of interfaces (as shown in Fig. 6a).

Nanotowers without SiO₂ interlayers were also prepared. As shown in Figure 6a, the activities of nanotowers with seven interfaces were close even though they had a different number of Au layers. In studying nanotowers with one interface (one bi-layer Au/CeO₂) and three interfaces (two bi-layers Au/CeO₂), it was found that although the activity increases with the number of interfaces, the response was not exactly in line with the larger number of interfaces. This indicates that nanotowers with more than four layers of film would form interfaces with similar properties so that the activity increases with the number of interfaces linearly. However, the properties of the first several layers are different from subsequent ones, whether deposited alone or as initial layers in the multilayer system. The local structure of the film will be investigated to understand this difference.

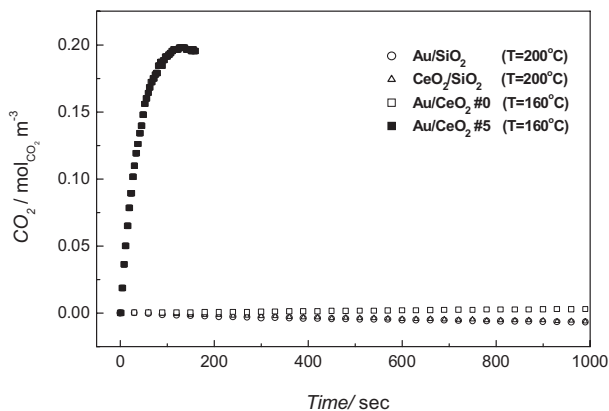


Figure 5. CO oxidation activity tests of various nanotower structures, with film thickness 4.5 nm layer⁻¹ for both Au and CeO₂.

CO was found (Fig. 5). The fact that only the Au/CeO₂ interface is active toward CO oxidation indicates that the active site is at the interface. The experiment demonstrates that the layers in the structure are and remain well separated. Thin films deposited on room temperature substrates are highly stressed,^[25] but can be relaxed under heating. Note that the deformation is most severe at the edge of the film, where the force is poorly balanced. However, if during reaction, the edge had been distorted and resulted in the mixing together of Au and CeO₂, it would form an active interface, and catalytic activity will be observed. Since this is not the case, it is believed that the edges of nanotowers are unmixed and maintained under the reaction conditions, which proves again that the particles across the edge found by TEM (see Fig. 3d) are formed during ion beam milling.

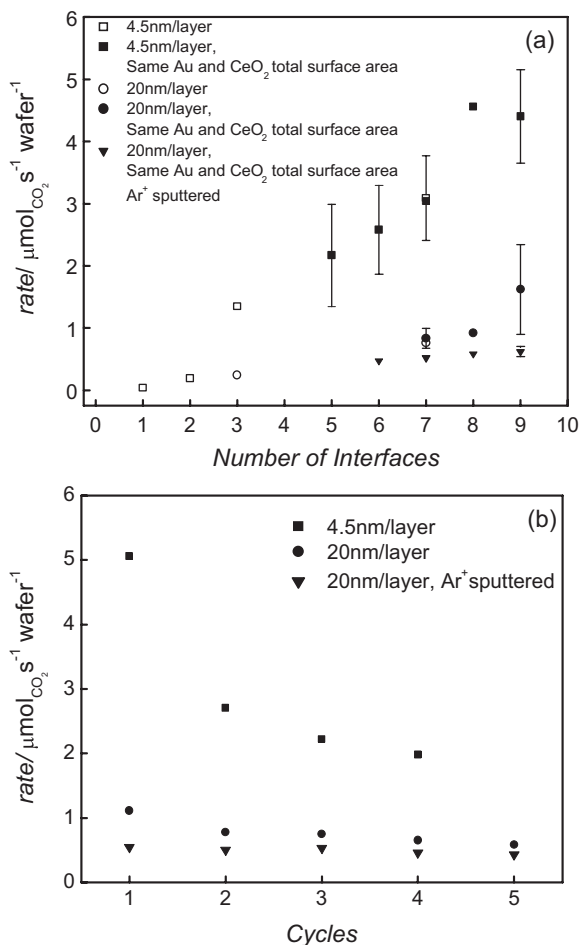


Figure 6. a) CO production rate normalized by catalyst on a 3" wafer; and b) stability of nanotowers with 9 active interfaces.

2.4. Effect of Nanolayer Thickness

Three samples with Au and CeO₂ layer thicknesses of 20 nm were prepared to investigate the effect of thickness. The 20 nm layer samples had seven, eight, and nine interfaces and a structure identical to that with 4.5 nm layers. The activity of the three samples, shown in Figure 6a, increases with the number of interfaces, but is ~50% of that of the nanotowers with 4.5 nm films. Since the interfacial length of the thick- and thin-layered structures shown in Figure 6a was the same, the difference in activity indicates a size contribution as well.

In view of these results, indicative of film thickness effect on the CO oxidation activity, additional sample characterization focused on the potential correlation of film strain with its thickness and reactivity. The variability of the microstrain, based on the (111) facets, varied considerably between the thin (4.5 nm) gold films and the thick ones (20 nm), from 1.9 to 0.4%, respectively. No appreciable difference between the corresponding CeO₂ layers was found. Hence, the difference in reactivity is attributed in part to the gold film microstrain. The effect is not linear, as the difference in activity (two-fold) is not commensurate with the microstrain difference (five-fold)

between the thin and thick-Au layered structures of Figure 6a. With time-on-stream, the activity of all nanotower structures decayed slowly. However, the activity of nanotowers with thick layers was found to decay more slowly than the thin layer samples (Fig. 6b).

Although the nanotower structure allows one to control the catalyst geometry better than a conventional particle catalyst, the orientation of the active surface, which is perpendicular to the substrate, limits the surface technology available to probe the local structure.

2.5. Modification of Edge Stress Using Low Energy Ar⁺ Bombardment

Low energy ion bombardment is sometimes applied to thin films after deposition to increase the film adhesion. For example, Ar⁺ ions would knock ions into trenches and voids, and transfer kinetic energy to the atoms that help them diffuse to a more stable location. As shown in TEM images, the Ar⁺ sputtered nanotower edges exhibit better thermal stability, which is believed to be due to release of the local stress at the edge. After sputtering off the edge by Ar⁺, the activity was lower by about one-third, but was more linear with the interfacial length (as shown in Fig. 6a). At the same time, the stability of the sample was enhanced (Fig. 6b).

These results show that microstrain is an important parameter affecting catalyst activity, and this is true in thin film-structures as well as in nanoparticles as has been reported in the recent literature.^[29] Highly strained gold films are more active for the CO oxidation reaction, while relaxation of the films with time-on-stream at 160 °C, can explain the observed gradual loss of activity.

3. Conclusions

Well-controlled and reproducible Au/CeO₂ nanotowers were prepared and used in studying the location of the active sites and the size effects in CO oxidation. The nanotowers with inserted SiO₂ layers breaking all the Au/CeO₂ interfaces showed no activity, indicating the stable unmixed layered structure at the edge of the nanotowers. The Au/CeO₂ interface was identified as the location of the active structures. The CO oxidation rate was found to scale with Au/CeO₂ interfacial length with the same structure.

TEM studies of the multilayers found uniform films and sharp interfaces between layers. XRD and artifacts in TEM image caused by FIB have identified that Au films were strained. The stress in the film is believed to affect the properties of the interface, and nanotowers with more strained thin (4.5 nm) films were more active than those with thick (20 nm) films. The importance of strain of the gold films, but not the ceria, shows that the active sites for this reaction are on gold. Ceria must then serve as a support that stabilizes these structures, something that silica cannot do. Nanotowers modified by low energy Ar⁺ bombardment were the least

active because the stress at the edge was partially relieved. However, the activity was stabilized upon reducing the stress of the film.

Although there are a number of issues in the nanotower structure that have not been fully resolved, the nanotower provides a controllable structure that can be used to quantitatively study the reaction with respect to the length of interface. Also, the nanotower structure could be easily adapted to study other supported Au catalysts.

4. Experimental

Catalyst Design: The Au/CeO₂ nanotower structure is designed to provide control of the three major structural variables that are believed to affect catalytic activity: surface area, interface length, and gold particle size. Varying each factor independently will allow one to observe corresponding changes in catalytic activity, and find answers to the following questions: (i) the location of the active sites; (ii) whether there is a quantitative relationship between activity and film properties; and (iii) whether there is a clear size effect due to Au.

The geometry of a nanotower is shown in Figure 1(a): the top layer is inert SiO₂ material, thus only the edge surface of the Au and CeO₂ layers is exposed. The thickness of the film simulates the particle size and interfaces are formed between neighboring Au and CeO₂ layers. The total surface area can be kept constant when the number of films and their thickness are fixed. However, the interface length can be varied quantitatively by inserting an inert layer between the Au and CeO₂ (as shown in Fig. 1b). Each inert layer inserted reduces the number of interfaces by one. Thus, one can eliminate any potential thickness effect due to Au. In studying the quantitative relationship between the activity and the active sites, a set of nanotowers was prepared by varying the number of interfaces from five to nine keeping the thickness and effective surface area unchanged. The selection of inert material is crucial. The candidate inert material should meet the following conditions: (i) the inert material should not be active for CO oxidation; (ii) no new active sites should be formed at the interface of Au or CeO₂ and the inert material; and (iii) The inert material should be easy to handle in an evaporation source and form a flat surface. Based on these requirements, SiO₂ was chosen to be the inert material.

To have enough catalyst for observable CO₂ conversion, 10⁷ nanotowers of the same structure were prepared on a silicon wafer (3" in diameter) using photolithography and vapor deposition. The activity of nanotowers listed in this paper is based on nanotowers per wafer unless otherwise mentioned.

Catalyst Preparation: The procedure of preparing nanotowers is shown schematically in Figure 2a, which includes photolithography, deposition and lift-off. A 3" p-type silicon wafer was used as substrate, and the top of the wafer was oxidized to SiO₂ (1000 Å) for better adhesion.

Prior to lithography, the wafer was dehydrated on a hot plate (130 °C, 30 min). It was then coated with photo resist (AZ[®] 5214-E, AZ Electronic Materials) using a spin-coater (3000 rpm, 0.4 min, Headway Research Inc.). The final thickness of the resist was approximately 2 μm, which was much thicker than the total thickness of the multilayers. The coated resist was dried in a furnace (85 °C, 30 min). The wafer was then exposed to the UV light (λ = 220–320, intensity 5–6, t = 10 s, MJB3, KarlSuss) through the contact mask, which defined the pattern. A post-exposure bake (85 °C, 30 min) was applied to fully activate the resist. The pattern was then reversed by a flood exposure with UV light. Finally, the pattern was developed in developer (AZ-422, AZ Electronic Materials USA Corp.). The intensity of UV light was reduced when passing through the resist starting at the surface, therefore formed the over-hanging shape as described in Figure 2a, preventing the edge of nanotower from touching the photoresist. The over-hang was further enhanced during deposition by the incident

atoms, resulting in gradually reducing the size of the opening of the well; therefore, the edge of the nanotowers was slightly tilted inward. However, the difference from the vertical shape was too small to affect the film thickness and the calculated interfacial length. The pattern was examined under an optical microscope to ensure the shape and size of the well were appropriate before use.

Deposition was conducted in a high vacuum e-beam chamber (E-beam, PAK-8, Sloan) with four source pockets. Pellet Au (99.99%), CeO₂ (99.99%, AITHACA Chemical Corp.), and SiO₂ (99.99%, Alfa Aesar) were used as source. The base pressure was 10⁻⁶ Torr, and the deposition rates were 1 Å s⁻¹ for all films. A crystal monitor (QT 7160, Fil-Tech Inc.) placed close to the substrate was used to measure the film thicknesses. No trace oxygen and no in situ annealing were used during the deposition.

Acetone was used to dissolve photoresist during the lift-off step. Accordingly, samples after deposition were immersed in acetone until the photo-resist was dissolved, the sample was then switched to clean acetone solution, and ultrasonicated for about 1 min. The sample was further rinsed in running DI water for 1 min to remove any solvent residue, and blow-dried with N₂. Before being tested for catalytic activity, each sample was examined under the optical microscope to check the complete removal of the photo-resist.

Characterization of the Film Structure: Film roughness of Au and CeO₂ films was studied using atomic force microscopy (AFM, NanoScope). The roughness was evaluated with the root mean square average of height deviation (R_q), defined by:

$$R_q = \sqrt{\frac{\sum Z_i^2}{n}} \quad (1)$$

where Z_i is the surface height deviation measured from the mean plane.

X-ray diffraction (XRD, Rigaku RU300, Kα) was used to examine the film structure. The film grain size was calculated using the Scherrer equation, and the film microstrain was evaluated using the single line method by analyzing the line broadening.[23]

Bright field TEM was conducted on JEOL-2011 of the film local structure. A cross-sectional specimen was prepared with both Small Angle Cleavage Technique (SACT)[24] and focused ion beam (FIB) cutting. SACT[24] only involves use of mechanical force, which is believed to avoid artifacts. However, it is hard to sample the edges because the sampling site is quite random. Also, the application was limited by the film adhesion between adjacent layers. The other preparation method used a FIB (FIB JEOL JEM-9320), which uses a high-energy Ga⁺ beam to cut out a specific site of the sample. The specimen prepared from FIB was compared with the specimen prepared from SACT in order to interpret the information correctly.

Catalytic Activity Measurements: The activity tests for CO oxidation were performed in a cold-wall recycle reactor (483 mL total volume). The wall of the reactor was water cooled to 20 °C in order to suppress any background reaction from the stainless steel walls. The wafer was placed on a plate heater inside the reactor and heated to desired temperatures. The reaction gas stream contained 1% CO and 2% O₂, balanced with He. The exit gas stream was sampled continuously by a quadrupole mass spectrometer (QMS) (Dycor 200, AMETEK) using a 50 μm, 1 m, quartz capillary to connect the atmospheric pressure reactor to the vacuum chamber of the QMS. Initial reaction rates were calculated by fitting the gas concentration–time curve. The sample was heated to 160 °C for 20 min in He, and the reactants were introduced sequentially by syringe injection. The reactor behaves as a well-mixed system relative to reaction times. No other pretreatment was applied. The sample was activated in the reactant gas mixture, usually in less than 30 min. The kinetic data were recorded three times at each temperature after the reaction rate became stable.

Modification of Film Edge with a Low Energy Ar⁺ Beam: Ion bombardment was used to modify the edge structure of some of the nanotowers. In addition to sputtering away the surface atoms, the ion

beam can change the film structure in two ways: (i) knocking adatoms into voids of the film; and (ii) increasing the diffusivity of the atoms by transferring of kinetic energy. The ion beam bombardment was conducted on fresh deposited samples in a RIE chamber (40 Torr Ar, 200 W, 25 min). The sputtering direction was normal to the surface; hence, the slightly tilted edge could be sputtered off. The activity of the modified nanotowers was tested under the same reaction conditions.

Received: January 06, 2008

Revised: June 19, 2008

Published online: September 1, 2008

-
- [1] M. A. Bollinger, M. A. Vannice, *Appl. Catal. B* **1996**, *8*, 417.
[2] G. J. Hutchings, M. Haruta, *Appl. Catal. A* **2005**, *291*, 2.
[3] M. Haruta, T. Kobayashi, H. Sano, N. Yamada, *Chem. Lett.* **1987**, *4*, 405.
[4] H. Y. Y. Ko, M. Mizuhata, A. Kajinami, S. Deki, *Thin Solid Films* **2005**, *491*, 86.
[5] M. Okumura, S. Nakamura, S. Tsubota, T. Nakamura, M. Azuma, M. Haruta, *Catal. Lett.* **1998**, *51*, 53.
[6] N. Lopez, T. V. W. Janssens, B. S. Clausen, Y. Xu, M. Mavrikakis, T. Bligaard, J. K. Nørskov, *J. Catal.* **2004**, *223*, 232.
[7] K. Okazaki, S. Ichikawa, Y. Maeda, M. Haruta, M. Kohyama, *Appl. Catal. A* **2005**, *291*, 45.
[8] Z. Yan, S. Chinta, A. A. Mohamed, J. P. Fackler, D. W. Goodman, *J. Am. Chem. Soc.* **2005**, *127*, 1604.
[9] C. T. Campbell, *Science* **2004**, *306*, 234.
[10] M. S. Chen, D. W. Goodman, *Science* **2004**, *306*, 252.
[11] G. J. Hutchings, M. S. Hall, A. F. Carley, P. Landon, B. E. Solsona, C. J. Kiely, A. Herzing, M. Makkee, J. A. Moulijn, A. Overweg, *J. Catal.* **2006**, *242*, 71.
[12] M. M. Schubert, S. Hackenberg, A. C. van Veen, M. Muhler, V. Plzak, R. J. Behm, *J. Catal.* **2001**, *197*, 113.
[13] T. Minato, T. Susaki, S. Shiraki, H. S. Kato, M. Kawai, K-i. Aika, *Surf. Sci.* **2004**, *566–568*, 1012.
[14] N. Lopez, J. K. Nørskov, T. V. W. Janssens, A. Carlsson, A. Puig-Molina, B. S. Clausen, J.-D. Grunwaldt, *J. Catal.* **2004**, *225*, 86.
[15] Q. Fu, H. Saltsburg, M. Flytzani-Stephanopoulos, *Science* **2003**, *301*, 935.
[16] Q. Fu, A. Weber, M. Flytzani-Stephanopoulos, *Catal. Lett.* **2001**, *77*, 87.
[17] M. Valden, X. Lai, D. W. Goodman, *Science* **1998**, *281*, 1647.
[18] M. Haruta, *Catal. Today* **1997**, *36*, 153.
[19] J.-D. Grunwaldt, A. Baiker, *J. Phys. Chem. B* **1999**, *103*, 1002.
[20] J. C. Frost, *Nature* **1988**, *334*, 577.
[21] I. Zuburtikudis, H. Saltsburg, *Science* **1992**, *258*, 1337.
[22] M. Chaplin, *Ph. D. Thesis*, University of Rochester, USA **1997**.
[23] T. H. DeKeijser, J. I. Langford, E. J. Mittemeijer, A. B. P. Vogels, *J. Appl. Crystallogr.* **1982**, *15*, 308.
[24] S. D. Walck, J. P. McCaffrey, *Thin Solid Films* **1997**, *308–309*, 399.
[25] D. L. Smith, *Thin-Film Deposition: Principles & Practice*, McGraw-Hill, New York, USA **1995**, Ch. 5.
[26] Y. Xu, M. Mavrikakis, *J. Phys. Chem. B* **2003**, *107*, 9298.
[27] M. Mavrikakis, B. Hammer, J. K. Nørskov, *Phys. Rev. Lett.* **1998**, *81*, 2819.
[28] S. Giorgio, C. R. Henry, B. Pauwels, G. van Tendeloo, *Mater. Sci. Eng. A* **2000**, *297*, 197.
[29] R. Si, M. Flytzani-Stephanopoulos, *Angew. Chem, Int. Ed.* **2008**, *47*, 2884.
-